Gaseous $H_5P_2O_8^-$ Ions: A Theoretical and Experimental Study on the Hydrolysis and Synthesis of Diphosphate Ion

Federico Pepi,[a] Andreina Ricci,*[a] Marzio Rosi,[b] and Marco Di Stefano[b]

Abstract: The structure and reactivity of gaseous $H_5P_2O_8^-$ ions obtained from the chemical ionization (CI) of an $H_4P_2O_7/H_2O$ mixture and from electrospray ionization (ESI) of $CH_3CN/H_2O/H_4P_2O_7$ solutions were investigated by Fourier transform ion cyclotron (FTICR) and triple quadrupole mass spectrometry. Theoretical calculations performed at the B3LYP/6-31+G* level of theory and collisionally activated dissociation (CAD) mass spectrometric results allowed the ionic population obtained in the CI conditions to be structurally characterized as a mixture of gaseous $[H_3P_2O_7\cdots H_2O]^-$, $[H_3PO_4\cdots H_2PO_4]^-$, and $[PO_3\cdots H_3PO_4\cdots H_2O]^-$ clusters. The energy profile emerging from theoretical calculations affords insight into the mechanism of diphosphate ion hydrolysis and synthesis.

Keywords: ab initio calculations · cluster compounds · diphosphate anions · gas-phase chemistry · mass spectrometry · phosphorus

Introduction

The hydrolytic cleavage of phosphate ester bonds is an essential and ubiquitous reaction in biological systems.[1] Intensive and continuous research efforts[2–18] have been made to study the hydrolysis mechanism of phosphate esters. These investigations have been focussed on gaining insight into the little-understood mechanistic aspects of important biological pathways such as those by which energy is stored and transferred in living cells or those responsible for enzyme regulation. The main debate is focused on the determination of the dominant mechanism of phosphate hydrolysis in aqueous solution, that is, whether it follows an associative or a dissociative mechanism. The dissociative mechanism involves proton transfer from the phosphoryl group to the oxygen-bridged atom and proceeds by the formation of a metaphosphate (PO_3^-) ion. The associative mechanism requires the formation of an intermediate or a transition state with a pentacoordinate phosphorus atom.

[a] Prof. F. Pepi, Prof. A. Ricci
Dip.to di Studi di Chimica e Tecnologia delle Sostanze Biologicamente Attive
Università di Roma "La Sapienza", P.le A. Moro, 5 00185 Rome (Italy)
Fax: (+39) 064-991-3602
E-mail: andreina.ricci@uniroma1.it

[b] Prof. M. Rosi, Dr. M. Di Stefano
Istituto per le Tecnologie Chimiche e Centro di Studi CNR "Calcolo Intensivo in Scienze Molecolari"
c/o Dipartimento di Chimica, Università di Perugia
Via Elce di Sotto 8, 06123 Perugia (Italy)

Physical-organic studies have provided extensive evidence for both the associative and dissociative mechanisms underlying phosphomonoesters' nonenzymatic reactions.[5] Computational studies have produced evidence in favor of both mechanistic alternatives for the nonenzymatic hydrolysis of monophosphate ester. Ab initio theoretical methods coupled to Langevin dipoles (LD) and polarized continuum (PCM) solvent methods have indicated that the barriers to associative and dissociative pathways are similar.[6] This conclusion was challenged by Hu and Brinck,[7] who determined the importance of the first solvation shell when they studied the hydrolysis of the $CH_3OPO_3H^-$, $CH_3OPO_3H^-\cdot H_2O$, and $CH_3OPO_3H^-\cdot(H_2O)_2$ species using high-level ab initio and density functional theory (DFT) methods coupled with the polarizable continuum model (PCM). The dissociative mechanism, which proceeds via a six-membered-ring transition state involving the water molecule, is found to be favored more than the associative mechanism, in both the gas and solution phase. In agreement with previous theoretical results,[8] DFT calculations carried out using the hybrid functional B3LYP on the dissociative hydrolysis reaction of $CH_3OPO_3H^-$ indicated that, in the gas phase, proton transfer to the methoxy group is concerted with P–O cleavage. The dissociative pathway of the $CH_3OPO_3^-\cdot H_2O$ ion is energetically favorable over the dissociative pathway of $CH_3OPO_3H^-$ only when the added water molecule plays an active catalytic role in forming the $CH_3O^+(H)PO_3^{2-}$ ion. The collapse of the hydrated tautomeric $CH_3O^+(H)PO_3^{2-}\cdot H_2O$ ion is rate-determining and may occur via a very short-lived metaphosphate intermediate or by a concerted S_N2-like displacement via a loose metaphosphate-like

  DOI: 10.1002/chem.200400293

transition state. This study does not allow any distinction to be made between these two alternatives. The existence of zwitterionic species was recently criticized by a theoretical study on the nonenzymatic hydrolysis of monophosphate and triphosphate ($TME(H)^{3-}$) esters performed using hybrid density functional methods.[2] For the monophosphate and triphosphate esters the dissociative pathway in the gas phase was found to be favored much more than the associative pathway. The active participation of a local water molecule lowers the activation energy of the dissociative mechanism for both the monophosphate and triphosphate esters.[2]

An alternative route proposed[6,7,9] for the hydrolysis of phosphate monoester monoanions is the substrate-assisted general base catalysis mechanism, which involves protonation of the reactant by a water molecule followed by nucleophilic attack of the hydroxide ion to form a pentacoordinate intermediate. This proposal has been criticized and disproved.[10,11]

As far as we know, there are neither direct experimental data nor independent theoretical results on the gas-phase hydrolysis mechanism of the diphosphate monoanion. All the theoretical studies on $H_4P_2O_7$, its anions, and their complexes with singly and doubly charged metal ions focussed their attention on the heat of the hydrolysis reaction. Gas-phase calculations on pyrophosphoric acid hydrolysis indicate that the reaction is almost thermoneutral and favored by solvation effects.[12] Gas-phase hydrolysis of the $H_3P_2O_7^-$ ion is endothermic and the enthalpy change decreases with increasing negative charge in the $H_2P_2O_7^{2-}$ and $HP_2O_7^{3-}$ species, owing to the greater internal electrostatic repulsion.[13] Multiply charged anions such as $HP_2O_7^{3-}$ and $P_2O_7^{4-}$ were hypothesized to be unstable in the gas phase, though Mg^{2+} complexation allows them to exist.[14] For the acid-catalyzed hydrolysis of pyrophosphate the potential energy surface is found to be dissociative if the bridging oxygen atom is protonated.[15] A possible catalytic role of the Mg^{2+} ion in the hydrolysis reaction of Mg–pyrophosphate complexes was investigated theoretically.[15–17]

Recently[18] we reported an experimental and theoretical study on the gas-phase ion chemistry of the inorganic diphosphate ion $H_3P_2O_7^-$, the simplest compound containing the P–O–P bond, which, at least in principle, could represent a model for understanding the factors controlling hydrolysis of phosphate linkage esters in living organisms. In this study the joint application of mass spectrometric techniques, electrospray ionization Fourier transform ion cyclotron resonance (ESI-FTICR), and triple quadrupole mass spectrometry (TQ-MS), as well as theoretical methods, provided information on the dissociative processes of diphosphate anions in the gas phase.

Herein, using the same integrated approach, we investigated the structure and reactivity of gaseous $H_5P_2O_8^-$ ions obtained from the chemical ionization (CI) of $H_4P_2O_7/H_2O$ gaseous mixtures and from electrospray ionization of $CH_3CN/H_2O/H_4P_2O_7$ solutions. The joint application of experimental and theoretical methods allows the gas-phase ion chemistry of $H_5P_2O_8^-$ ions to be investigated and insight to be gained into the gas-phase hydrolysis and synthesis of the diphosphate ion.

Results

$H_5P_2O_8^-$ ions were obtained in the source of the FTICR mass spectrometer from electrospray ionization of a solution of $H_4P_2O_7$ or H_3PO_4 in CH_3CN/H_2O (1:1).[18] These ions are not detected in CH_3CN/H_2O (1:1) ESI solutions of $Na_4P_2O_7$ and $Na_5P_3O_{10}$. In the source of the triple quadrupole mass spectrometer, the $H_5P_2O_8^-$ ions are formed from the CI/CH_4 of $H_4P_2O_7$ in the presence of H_2O or from the CI/CH_4 of H_3PO_4.

In principle, a number of structural isomers correspond to the $H_5P_2O_8^-$ molecular formula: $[H_3P_2O_7\cdots H_2O]^-$ (**I**), $[H_5P_2O_8]^-$ (**II**), $[H_3PO_4\cdots H_2PO_4]^-$ (**III**), and $[H_3PO_4\cdots PO_3\cdots H_2O]^-$ (**IV**).

Ion **II** represents the linear $H_5P_2O_8^-$ ions resulting from the direct addition of water to diphosphoric acid and involves a pentacoordinated P atom. All the other species are characterized by cluster structures in which electrostatic interactions hold together $H_3P_2O_7^-$ and water (**I**), $H_2PO_4^-$ and phosphoric acid (**III**), or PO_3^-, water, and a phosphoric acid molecule (**IV**).

The existence of cluster **IV** is hypothesized by analogy with our previous investigation[18] of gaseous $H_3P_2O_7^-$ ions, which suggests the possible presence of the isomeric $[H_3PO_4\ PO_3]^-$ cluster together with the linear diphosphate ion in the ionic population characterized by the ratio at m/z 177.

According to this hypothesis, clusters **I** and **IV** could be formed from Reactions (1) and (2) through the direct addition of a water molecule to the ions at m/z 177:

$$\underset{}{H_3P_2O_7^- + H_2O \rightarrow} \underset{\mathbf{I}}{[H_3P_2O_7\cdots H_2O]^-} \quad (1)$$

$$\underset{}{[H_3PO_4\cdots PO_3]^- + H_2O \rightarrow} \underset{\mathbf{IV}}{[H_3PO_4\cdots PO_3\cdots H_2O]^-} \quad (2)$$

Moreover, cluster **III** could reasonably be generated from Reaction (3) when pyrophosphoric acid is replaced by phosphoric acid under both the TQ and FTICR conditions:

$$\underset{}{H_2PO_4^- + H_3PO_4 \rightarrow} \underset{\mathbf{III}}{[H_2PO_4\cdots H_3PO_4]^-} \quad (3)$$

ESI/FT-ICR experiments: The $H_5P_2O_8^-$ ions generated from $H_4P_2O_7$ and H_3PO_4 ESI solutions were isolated and structurally characterized by CAD experiments. Their reactivity toward many compounds was investigated. In the FT-ICR CAD experiments, the $H_5P_2O_8^-$ ions were transferred into the cell, isolated by soft ejection techniques, and allowed to collide with argon after translational excitation by a suitable radio frequency pulse. The CAD spectra of $H_5P_2O_8^-$ ions obtained from both the pyrophosphoric and phosphoric acid solutions displayed the PO_3^- fragment at m/z 79, the $H_2PO_4^-$ fragment at m/z 97 (corresponding to the loss of an H_3PO_4 molecule), and the fragment at m/z 177 (corresponding to the loss of a water molecule).

Under the low-pressure conditions of the FT-ICR experiments (10^{-7}–10^{-8} mbar), the $H_5P_2O_8^-$ ions were inert toward several compounds such as H_2O, alcohols (CH_3OH, C_2H_5OH, CF_3CH_2OH), and ketones (CH_3COCH_3). From their reaction with CF_3COOH ($\Delta H°_{acid} = 323\,kcal\,mol^{-1}$), besides the CF_3COO^- ion (*m*/*z* 113) and the $H_2PO_4^-$ ion (*m*/*z* 97), an ion at *m*/*z* 211, which reasonably corresponded to the $[H_2PO_4 + CF_3COOH]$ addition product, was detected.

To verify the possible formation of the ion at *m*/*z* 195 by Reactions (1) and (2), the $H_3P_2O_7^-$ ions at *m*/*z* 177, generated in the ESI source of the ICR spectrometer, were transferred to the resonance cell and allowed to react with H_2O. As previously reported[18] under low-pressure FT-ICR conditions, the $H_3P_2O_7^-$ ions do not react with H_2O.

TQ/MS experiments: The CAD spectrum of the $H_5P_2O_8^-$ ion at *m*/*z* 195 (obtained from CI/CH_4 of pyrophosphoric acid and water) recorded at nominal collision energies ranging from 0 to 50 eV (laboratory frame) is reported in Figure 1. It should be noted that, irrespective of its origin, the CAD spectrum of the ion at *m*/*z* 195 obtained from the CI/CH_4 of phosphoric acid is identical.

The spectrum displays two fragmentation channels, forming ions at *m*/*z* 177 and *m*/*z* 97, which correspond to the loss of a water and a phosphoric acid molecule, respectively. The

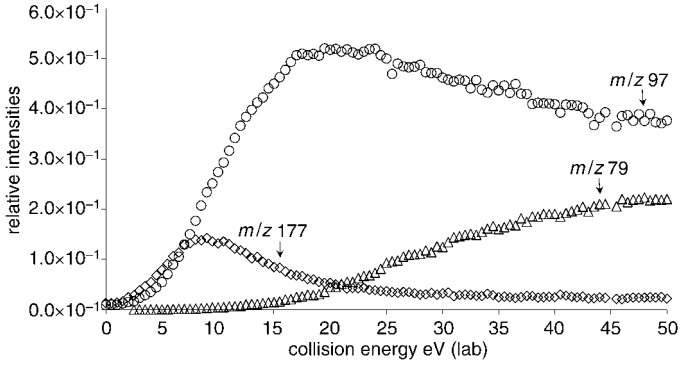

Figure 1. Energy-resolved TQ/CAD spectrum of the $H_5P_2O_8^-$ ions at *m*/*z* 195 from $H_4P_2O_7/H_2O/CH_4$/CI. The intensity profile of the parent ion is not shown.

low dissociation energy of the ion at *m*/*z* 177 suggests the loss of a water molecule from a loosely bound ion complex such as the $[H_3P_2O_7\cdots H_2O]^-$ cluster **I** or the $[H_3PO_4\cdots PO_3\cdots H_2O]^-$ cluster **IV**. The fragment at *m*/*z* 97 appears at a slightly higher collision energy and could arise from the $[H_3PO_4\cdots H_2PO_4]^-$ clusters, **III** or from the $[H_3PO_4\cdots PO_3\cdots H_2O]^-$ clusters **IV** following the loss of the H_3PO_4 moiety.

To obtain additional information, labeled $H_5P_2O_6{}^{18}O$ ions at *m*/*z* 197 were generated by introducing $H_2{}^{18}O$ into the ion source. The CAD spectrum of the $H_5P_2O_6{}^{18}O$ ions taken at a collision energy of 30 eV (laboratory frame) shows that the fragment ion at *m*/*z* 177 shifts almost entirely to *m*/*z* 179, indicating the loss of an unlabeled water molecule. In addition, the ion at *m*/*z* 97 splits into two fragments of comparable intensity at *m*/*z* 97 and *m*/*z* 99, indicating the loss of both labeled and unlabeled phosphoric acid. In order to seek further evidence, the $H_3P_2O_7^-$ ions were allowed to react with CH_3OH in the ion source. Figure 2 shows the

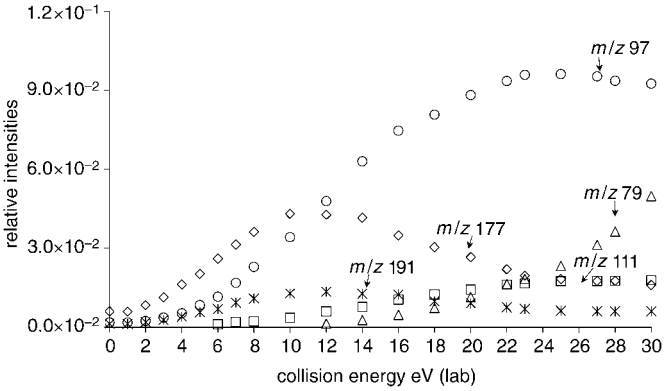

Figure 2. Energy-resolved TQ/CAD spectrum of the $[H_3P_2O_7 + CH_3OH]^-$ ions at *m*/*z* 209 from $H_4P_2O_7/CH_3OH/CH_4$/CI. The intensity profile of the parent ion is not shown.

CAD spectrum of the $[H_3P_2O_7 + CH_3OH]^-$ addition product at *m*/*z* 209, recorded at nominal collision energies ranging from 0 to 30 eV (laboratory frame). The fragment ions at *m*/*z* 191, 177, and 111 correspond to the loss of a water, methanol, and phosphoric acid molecule, respectively. Interestingly, the fragment ion at *m*/*z* 97 results from the loss of a methylphosphate molecule.

The assignment of these fragments was validated by the use of labeled $CH_3{}^{18}OH$ to generate the $[H_3P_2O_7 + CH_3{}^{18}OH]^-$ ions at *m*/*z* 211. The CAD spectrum shows fragments at *m*/*z* 193, 113, 97, and 177, confirming the loss of unlabeled water, phosphoric acid, $CH_3{}^{18}OPO_3H$, and $CH_3{}^{18}OH$, respectively. To verify the possibility of the occurrence of Reaction (1), the $H_3P_2O_7^-$ ions were isolated in the ion source of the TQ mass spectrometer and were allowed to react with H_2O in the hexapole cell. The addition product at *m*/*z* 195 is observed, as well as the ion at *m*/*z* 209 when methanol is used instead of water.

The loss of an unlabeled water molecule (fragment at *m*/*z* 179) in the CAD spectrum of the $[H_3P_2O_7 + H_2{}^{18}O]$ ions (*m*/*z* 197) and the loss of a water molecule (fragment at *m*/*z* 191) in the CAD spectrum of the $[H_3P_2O_7 + CH_3OH]$ ions (*m*/*z* 209) both indicate the occurrence of isomerization processes that lead to the formation of complexes incorporating the labeled water (or methanol) molecule into the moiety being lost as a charged fragment. However, isomerization processes are responsible for the formation of the same ionic population from CH_4/CI of both pyrophosphoric and phosphoric acid.

Theoretical results: At the B3LYP/6-31+G* level of theory, the study of the $H_5P_2O_8^-$ potential energy surface leads to the characterization of numerous structural isomers of the species of interest. In particular, in accordance with the ex-

perimental hypothesis, four different groups of anions (**I**–**IV**), may be optimized with either a linear or a cluster geometry. They will be described separately and within every group each isomer will be named by using the group number followed by a letter assigned on the basis of mechanistic rather than energetic considerations.

In Table 1 we report the thermochemical parameters at the B3LYP/6–31+G* level of theory for the isomerization processes of interest, the most significant of which are schematically represented in Figures 9, 10, 11. In Figure 4 we show the optimized geometries of the transition states involved in the isomerization processes considered. The dissociation energies are listed in Table 2.

Table 1. Thermochemical parameters at the B3LYP/6-31+G* level of theory for the isomerization processes among the investigated cations of formula $H_5P_2O_8^-$.

Reaction	ΔH [kcal mol^{-1}]	E_a [kcal mol^{-1}]
Ia→**Ib**	−4.3	–
Ia→**IIa**	26.7	34.8
Ia→**IVa**	14.5	44.1
Ib→**Ic**	3.5	–
Id→**Ia**	8.6	14.1
IIa→**IIb**	0.7	1.6
IIa→**Va**	−12.8	14.3
IIb→**IIIa**	−28.1	–
IIIa→**IIIb**	−3.2	–
IIIa→**IIIc**	−6.4	–
IIIa→**IVa**	15.2	32.9
$[PO_3^-\cdot\cdot H_2O]$→$H_2PO_4^-$	−9.2	17.1

The $[H_3P_2O_7^-\cdot\cdot H_2O]^-$ clusters, group I: Figure 3 displays the optimized geometries of the clusters formed by $H_3P_2O_7^-$ ions and an H_2O molecule, which are held together by electrostatic interactions. These are also labeled group **I**.

Cluster **Id** is the most stable member of the group. The H_2O molecule is coordinated to the diphosphate anion, previously[18] characterized as the lowest energy isomer on the potential energy surface of $H_3P_2O_7^-$ ions. Notably, the coordination of water does not bring about any noticeable changes in the fragment's geometry, apart from a different orientation of the terminal hydrogen atom.[18] By means of a barrier-free process, **Id** can eliminate the water molecule and produce the linear diphosphate monoanion. At our level of theory, an endothermicity of 13.3 kcal mol^{-1} was calculated (Table 2). By passing through **TS1** (Figure 4; Table 1), **Id** can give **Ia**. This process is endothermic by 8.6 kcal mol^{-1} and an activation barrier of 14.1 kcal mol^{-1} was computed. In **Ia** both the hydrogen atoms of the H_2O molecule are coordinated by electrostatic interactions to two oxygen atoms belonging to different monophosphate subunits. Geometry optimization gives a P-O-P angle of 127.5°. This structure can easily be broken down in a barrier-free process with the further release of the water molecule and the $H_3P_2O_7^-$ ion. We calculated this process to be endothermic by 15.4 kcal mol^{-1}.

The other clusters investigated include two structures, labeled as **Ib** and **Ic**, whose optimized geometries are given in Figure 3. As can be seen, not only do they differ in the spatial orientation of the water molecule, but also in the position of the H–O groups in the diphosphate skeleton. **Ib** is 4.3 kcal mol^{-1} lower in energy than **Ia**, and the loss of H_2O from **Ib** is a process that is endothermic by 9.3 kcal mol^{-1}. Finally, **Ic** is less stable than **Ib** by 3.5 kcal mol^{-1}. Indeed **Ia** and **Ic** are found to be isoenergetic, and the isomerization **Ia**→**Ic** is endothermic by only 0.8 kcal mol^{-1}, at least at our level of theory. The dissociation of **Ic** into $H_3P_2O_7^-$ and H_2O is a barrier-free process endothermic by 5.8 kcalmol^{-1}.

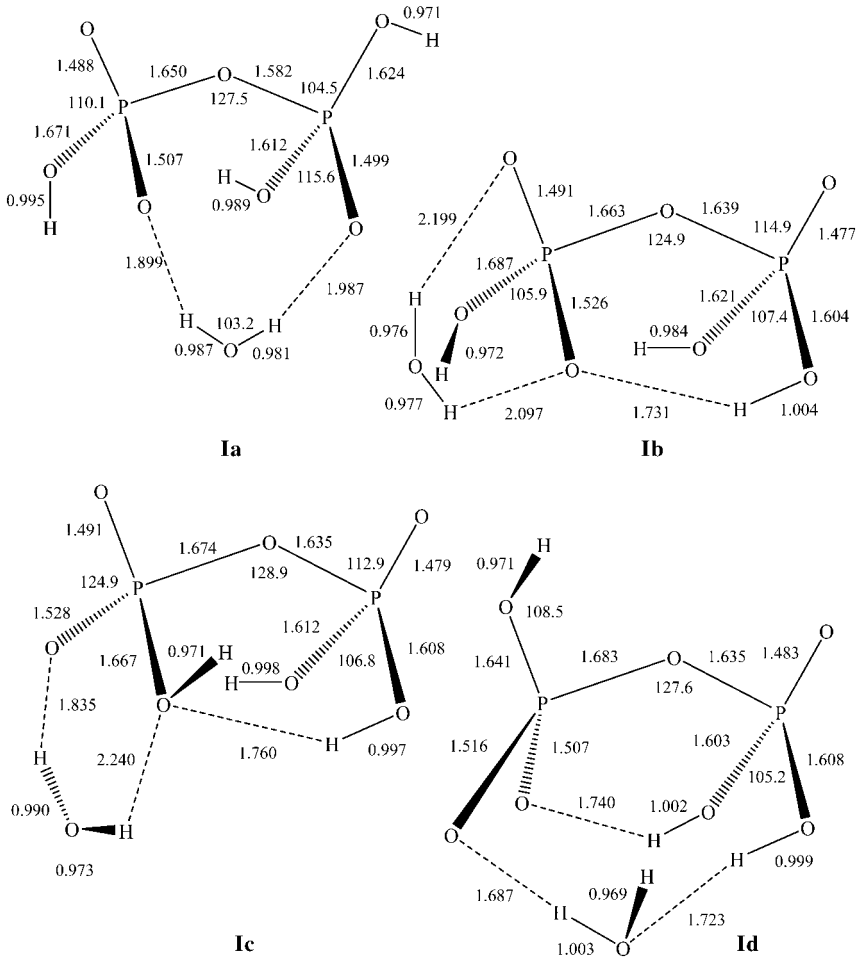

Figure 3. Optimized geometry at the B3LYP/6-31+G* level of theory of the $[H_3P_2O_7^-\cdot\cdot H_2O]^-$ cluster, group **I**. Bond lengths are in Å and angles in degrees.

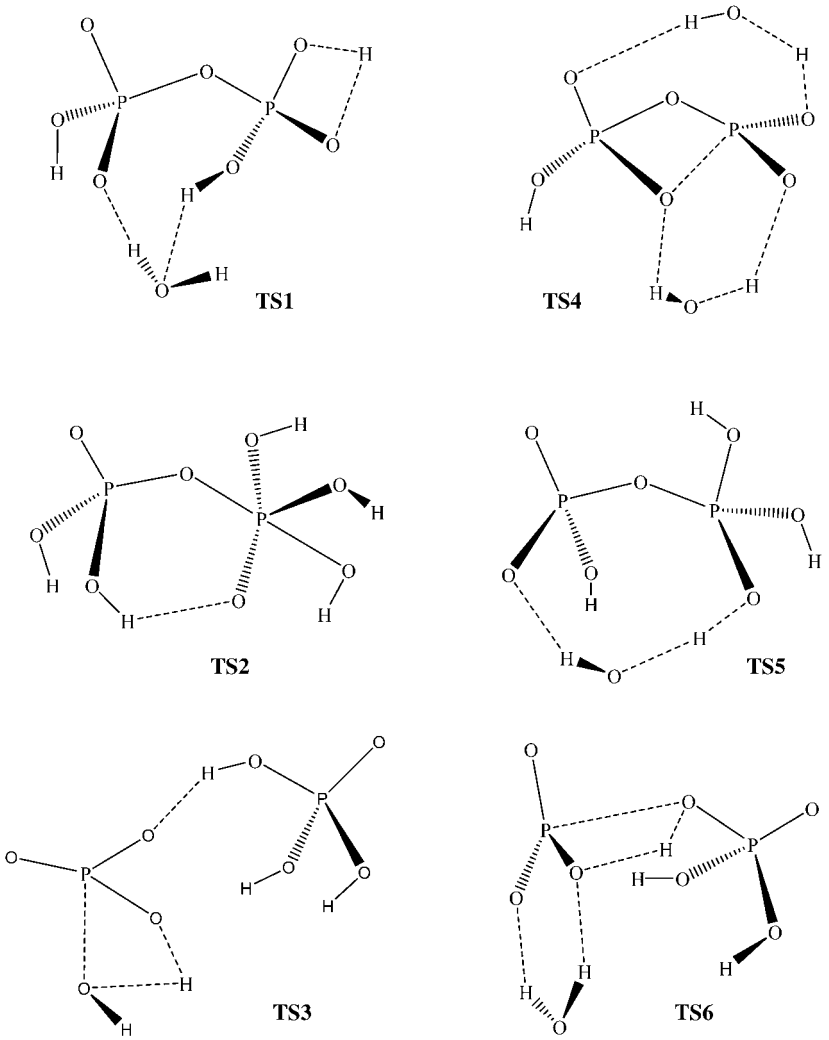

Figure 4. Schematic representation at the CCSD(T)/6-31+G* level of theory of the representative transition states for the potential energy surface under study.

Table 2. Thermochemical parameters at the B3LYP/6-31+G* level of theory for the fragmentation processes of interest.

Reaction	ΔH [kcal mol^{-1}]
Ia→$H_3P_2O_7^-+H_2O$	15.4
Ia→$HPO_3+H_2O+H_2PO_4^-$	68.4
Ib→$H_3P_2O_7^-+H_2O$	9.3
Ic→$H_3P_2O_7^-+H_2O$	5.8
Id→$H_3P_2O_7^-+H_2O$	13.3
IIb→$H_2PO_4^-+H_3PO_4$	4.9
IIIa→$H_2PO_4^-+H_3PO_4$	33.0
IIIb→$H_2PO_4^-+H_3PO_4$	29.8
IIIc→$H_2PO_4^-+H_3PO_4$	26.6
IVa→$H_3PO_4+[PO_3\cdots H_2O]^-$	27.0
IVa→$[H_3PO_4\cdots PO_3]^-+H_2O$	6.3
Va→$HP_2O_6^-+2H_2O$	18.4
Va→$[HP_2O_6\cdots H_2O]+H_2O$	7.2
$[PO_3\cdots H_2O]^-\rightarrow PO_3^-+H_2O$	13.9

The $H_5P_2O_8^-$ linear anions, group II: In Figure 5 we report the optimized geometries of the linear $H_5P_2O_8^-$ anions. In both of them, the pyrophosphate linkage P–O–P is preserved, although one of the phosphorus atoms has a pentacovalent nature. In **IIa**, the pentacovalent phosphorus is coordinated to four OH groups, in **IIb** to three OH groups. Apart from this difference, they both display stabilizing electrostatic interactions involving the hydrogen atoms of the OH groups and the oxygen atoms. In both structures, an appreciably elongated P–O bond of the P–O–P linkage is optimized. In **IIa**, the P–O bond involving the tetracovalent P is computed to have a length of 1.715 Å, while in **IIb** an even longer bond (1.772 Å) related to the pentacovalent phosphorus is found. This value might indicate the formation of a partial electrostatic bond. Thus, it is to be expected that **IIb** could break this weak interaction and evolve into the separate $H_2PO_4^-$ and H_3PO_4 species. No energy barrier is calculated for this process, at least at our level of theory. This fragmentation is slightly endothermic (4.9 kcal mol^{-1}). The isomerization **IIa**→**IIb** is endothermic by 0.7 kcal mol^{-1}. The B3LYP/6-31+G* geometry of the transition state for this process, labeled **TS2**, is given in Figure 4. The activation barrier of this process (1.6 kcal mol^{-1}) indicates that both anions can easily and rapidly isomerise into each other and are thus mutually interchangeable. Finally, on the production of **IIa** from the $[H_3P_2O_7\cdots H_2O]^-$ clusters, we optimized the transition structure labeled **TS5** for the isomerization **Ia**→**IIa**. This pathway is endothermic by 26.7 kcal mol^{-1} with an activation barrier of 34.8 kcal mol^{-1}.

The $[H_3PO_4\cdots H_2PO_4]^-$ clusters, group III: In Figure 6 we report the optimized geometries of the investigated clusters containing both the H_3PO_4 molecule and the $H_2PO_4^-$ ion, connected to each other by electrostatic interactions, also labeled group **III**.

As may be seen, they essentially differ by the spatial positions of the units that form them. The anion labeled **IIIa** can be directly produced from **IIb** in a barrier-free process and the isomerization **IIb**→**IIIa** is exothermic by 28.1 kcal mol^{-1}. The release of $H_2PO_4^-$ from **IIIa** is a barrier-free process and is endothermic by 33.0 kcal mol^{-1}. The cluster labeled **IIIb** has a more symmetric geometry, since the three electrostatic interactions connecting the H atoms of H_3PO_4 to the oxygen atom of $H_2PO_4^-$ are optimized. Cluster **IIIb** is more stable than **IIIa** by 3.2 kcal mol^{-1}. Finally, a third structure **IIIc** was investigated; it is more stable than **IIIa** by

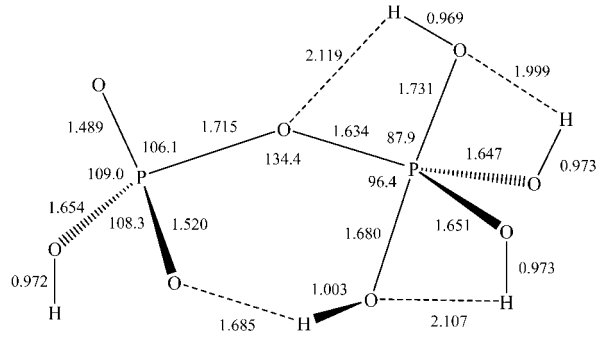

IIa

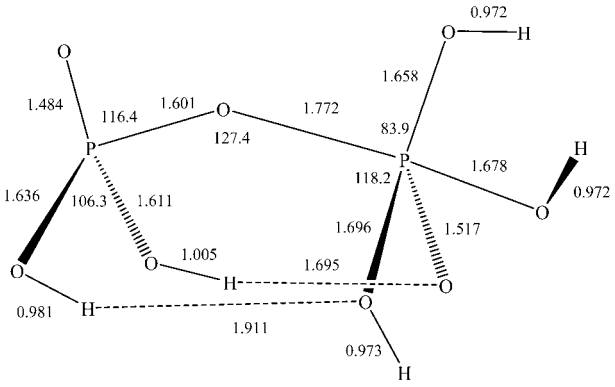

IIb

Figure 5. Optimized geometries at the B3LYP/6-31+G* level of theory of the $H_5P_2O_8^-$ ions group **II**. Bond lengths are in Å and angles in degrees.

6.4 kcal mol^{-1}. Cluster **IIIc** differs from **IIIb** mainly in the electrostatic interactions connecting the two phosphate moieties. Both fragments are spatially oriented so that they can form three interactions between the hydrogens of the OH groups and the oxygen atoms of the P–O bonds. On the release of $H_2PO_4^-$ and H_3PO_4 from both **IIIb** and **IIIc** at the B3LYP/6-31+G* level of theory we calculate that these processes are barrier-free and endothermic by 29.8 kcal mol^{-1} and 26.6 kcal mol^{-1}, respectively.

The $[H_3PO_4\cdots PO_3\cdots H_2O]^-$ clusters, group IV: In Figure 7 we report the optimized geometry at the B3LYP/6-31+G* level of theory of cluster **IVa** together with that of the hydrated metaphosphate anion here labeled $[PO_3\cdots H_2O]^-$. In **IVa** the H_3PO_4 molecule is electrostatically coordinated to both a PO_3^- ion and an H_2O molecule and this cluster is thought to be an additional source of the $H_2PO_4^-$ ion. In fact, $H_2PO_4^-$ is known to also be present in the form of a cluster structure in which the metaphosphate ion PO_3^- is coordinated to a water molecule.[15] Our calculations indicate that the formation of the hydrated metaphosphate ion $[PO_3\cdots H_2O]^-$ and H_3PO_4 from **IVa** is a barrier-free process that is endothermic by 27.0 kcal mol^{-1}. The $[PO_3\cdots H_2O]^-$ ion, once formed, can then isomerise to $H_2PO_4^-$. This process is exothermic by 9.2 kcal mol^{-1} with an energy barrier of 17.1 kcal mol^{-1}. Furthermore, $[PO_3\cdots H_2O]^-$ can also break its electrostatic interactions and release separate H_2O and PO_3^-. We calculate this process to be endothermic by 13.9 kcal mol^{-1}. In addi-

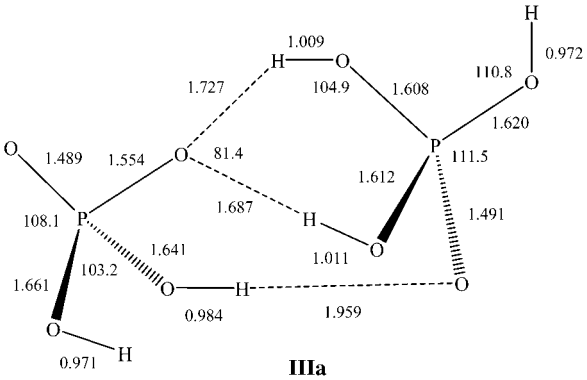

IIIa

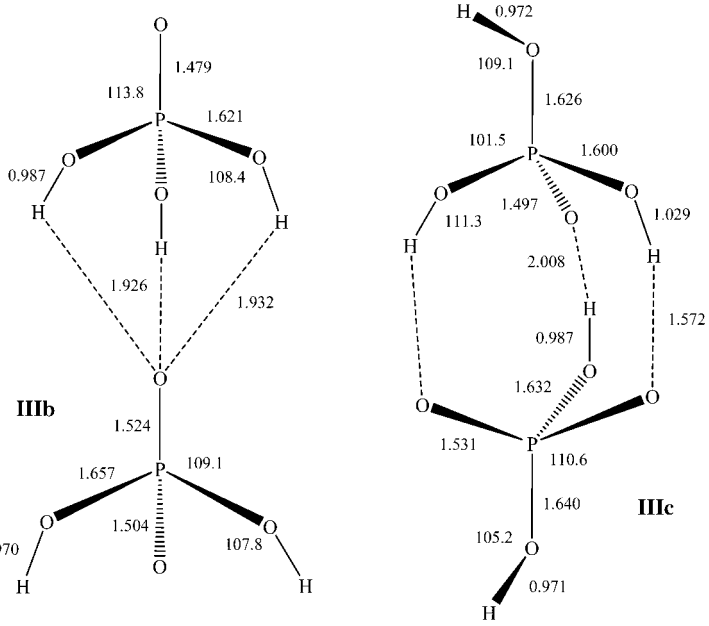

Figure 6. Optimized geometries at the B3LYP/6-31+G* level of theory of the $[H_3PO_4\cdots H_2PO_4]^-$ clusters, group **III**. Bond lengths are in Å and angles in degrees.

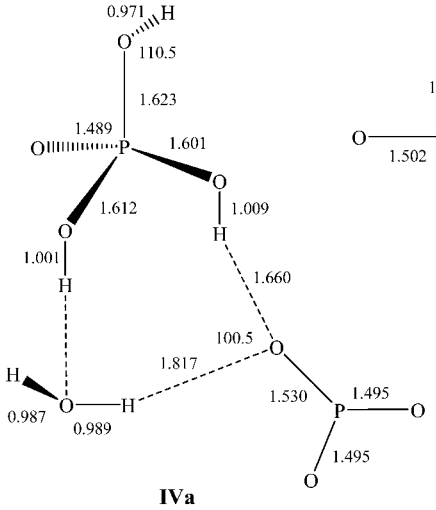

IVa

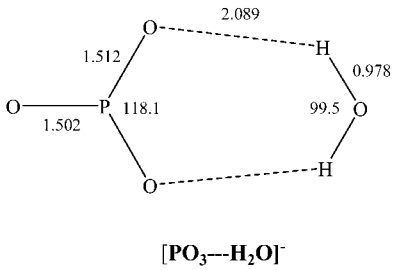

$[PO_3\cdots H_2O]^-$

Figure 7. Optimized geometries at the B3LYP/6-31+G* level of theory of cluster **IVa**, and of the hydrated metaphosphate anion, $[PO_3\cdots H_2O]^-$. Bond lengths are in Å and angles in degrees.

tion, **IVa** can release an H_2O molecule to produce the $[H_3PO_4\cdots PO_3]^-$ cluster whose optimized geometry has already been described.[18] For this species our calculations indicate an endothermicity of 6.3 kcal mol^{-1} with no activation barrier.

With regard to the formation of **IVa** from the previously described intermediates, the transformation **IIIa**→**IVa** is found to be endothermic by 15.2 kcal mol^{-1} with an activation barrier of 32.9 kcal mol^{-1}. The transition state **TS3** (Figure 4) is optimized in this process. Cluster **IVa** can also be obtained from **Ia** via the transition structure **TS6** (Figure 4). The thermochemical studies at our level of theory give a barrier height of 44.1 kcal mol^{-1} and an endothermicity of 14.5 kcal mol^{-1}.

The $[H_2O\cdots HP_2O_6\cdots H_2O]^-$ clusters, group V: By analogy with our previous investigation,[18] we may postulate the existence of a cyclic $HP_2O_6^-$ anion held together with two water molecules by electrostatic interactions. In Figure 8 we

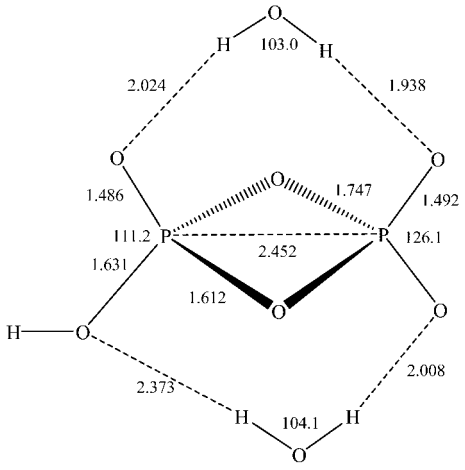

Va

Figure 8. Optimized geometries at B3LYP/6-31+G* level of theory of cluster **Va**. Bond lengths are in Å and angles in degrees.

report the B3LYP/6-31+G*-optimized geometry of cluster **Va**. As we can observe, the $HP_2O_6^-$ moiety is bound to two water molecules by electrostatic interactions involving the hydrogen atom of the H_2O molecules and the oxygen atoms of $HP_2O_6^-$. Cluster **Va** can be formed from **IIa** via the transition state labeled **TS4** (Figure 4). We calculate this isomerization as exothermic by 12.8 kcal mol^{-1} with an activation barrier of 14.3 kcal mol^{-1}. The release of a water molecule with the production of the electrostatically bound complex $[HP_2O_6\cdots H_2O]$[18] is endothermic by 7.2 kcal mol^{-1} and the loss of both water molecules endothermic by 18.4 kcal mol^{-1}.

Discussion

Two pieces of evidence concur in suggesting the presence of clusters **I** and **IV** in the ion population investigated by TQ mass spectrometry: 1) the fragment ion at *m*/*z* 177, corresponding to the loss of the H_2O moiety, appears at low collision energy values in the CAD spectrum of $H_5P_2O_8^-$, and 2) the formation of the $H_5P_2O_8^-$ ions in the hexapole cell from the reaction between water and the ion at *m*/*z* 177, previously characterized as having the linear $H_3P_2O_7^-$ and eventually the $[H_3PO_4\cdots PO_3]^-$ cluster structure.

Furthermore, three pieces of evidence clearly indicate the occurrence of isomerization processes: 1) the loss of unlabeled water from the ions at *m*/*z* 197, resulting from the addition of labeled water to the ions at *m*/*z* 177, 2) the loss of water and methylphosphate from the ions at *m*/*z* 209, resulting from the addition of methanol to the ions at *m*/*z* 177, and 3) the identity of the spectra of the $H_5P_2O_8^-$ ions obtained from CI/CH_4 of phosphoric acid or pyrophosphoric acid in the presence of water.

To rationalize the experimental results we used computational methods to investigate the isomerization pathways of the $[H_3P_2O_7\cdots H_2O]^-$ cluster **I** into the $[H_3PO_4\cdots H_2PO_4]^-$ cluster **III** and into the $[H_3PO_4\cdots PO_3\cdots H_2O]^-$ cluster **IV**. In particular, two possible pathways for the hydrolysis of the $H_3P_2O_7^-$ ions were considered, the so-called dissociative and associative mechanisms.

Figure 9 shows the energy profile of the associative hydrolysis of the diphosphate investigated at the B3LYP/6-31+G* level of theory. The linear $H_5P_2O_8^-$ phosphorane

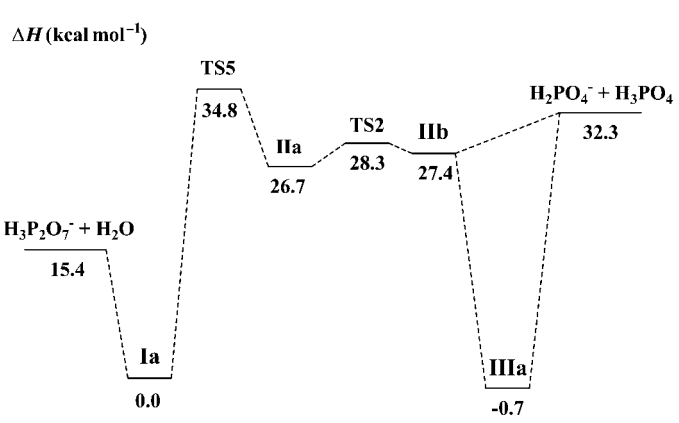

Figure 9. Schematic representation at the B3LYP/6-31+G* level of theory of the associative hydrolysis of diphosphate anions. All thermochemical parameters are given in kcal mol^{-1} and are calculated at 298.15 K.

ions, **IIa**, can be formed from the $[H_3P_2O_7\cdots H_2O]^-$ cluster **Ia** in a process that is endothermic by 26.7 kcal mol^{-1} and characterized by an activation barrier of 34.8 kcal mol^{-1}. By analysing the structure of the transition state **TS5** shown in Figure 4, the partial formation of both the P–O and O–H bonds may be observed together with the breaking of the electrostatic interactions binding the water molecule to the phosphate skeleton.

By shifting a proton **IIa** can isomerize to **IIb** via **TS2** (Figure 4). The P–O bond, already elongated in **IIb**, is definitively broken, leading to the formation of the

$[H_2PO_4\cdots H_3PO_4]^-$ cluster **IIIa**. This process is exothermic by 28.1 kcal mol^{-1} with no activation energy. Moreover, in a barrier-free dissociation process, **IIb** can evolve into the separate H_3PO_4 and $H_2PO_4^-$ species. This fragmentation is barrier-free and endothermic by 4.9 kcal mol^{-1}.

In Figure 10 we outline an alternative association pathway involving a different isomerization of **IIa**. We postulate this mechanism based on our previous results[18], which prove

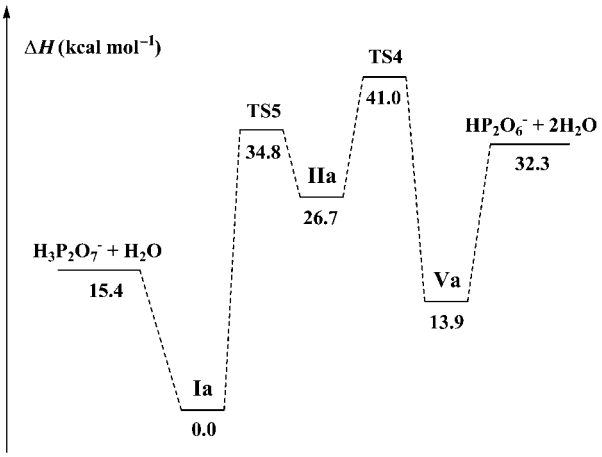

Figure 10. Schematic representation at the B3LYP/6-31+G* level of theory of the release of the water molecule by formation of cluster **IVa**. All thermochemical parameters are given in kcal mol^{-1} and are calculated at 298.15 K.

that the dimetaphosphate or cyclodiphosphate anion $HP_2O_6^-$ is formed from the induced dehydration of the diphosphate anion in the gas phase. Therefore, this investigation is aimed at ascertaining the possible release of a water molecule from an alternative pathway, requiring the formation of the $[H_2O\cdots HP_2O_6\cdots H_2O]^-$ cluster **Va**. As regards this mechanism, **IIa**, once formed, can evolve into **Va** by passing through **TS4**. At the B3LYP/6-31+G* level of theory we calculate an exothermicity of 12.8 kcal mol^{-1} and an activation barrier of 14.3 kcal mol^{-1}. Cluster **Va** is found to be 13.9 kcal mol^{-1} less stable than **IIa**. The release of a water molecule with the production of the electrostatically bound complex $[HP_2O_6\cdots H_2O]$[18] is computed to be endothermic by 7.2 kcal mol^{-1} and the loss of both water molecules is endothermic by 18.4 kcal mol^{-1}.

Our computational study of the dissociative hydrolysis mechanism was implemented by first considering the classic dissociative mechanism involving proton shift from an OH group to the O bridging atom. In Figure 11 we report the energy profile of the dissociative hydrolysis of $H_5P_2O_8^-$ ions investigated at the B3LYP/6-31+G* level of theory.

Isomerization **Ia**→**IVa** by the classical dissociation mechanism is endothermic by 14.5 kcal mol^{-1}. The optimized transition state is labeled **TS6** (Figure 4), which gives rise to a barrier height of 44.1 kcal mol^{-1}. In the transition state **TS6** (Figure 4), the partial formation of cluster **IVa** may be observed. The P–O–P linkage is broken to give the electrostatic interaction between the phosphoric acid and the metaphosphate anion. The hydrogen atom moving towards the

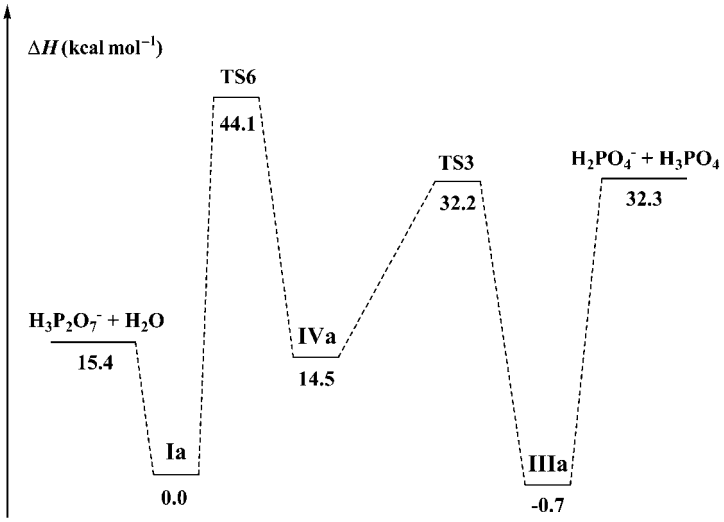

Figure 11. Schematic representation at the B3LYP/6-31+G* level of theory of the dissociative hydrolysis of diphosphate anions. All thermochemical parameters are given in kcal mol^{-1} and are calculated at 298.15 K.

oxygen of the $H_2PO_4^-$ moiety in order to give the H_3PO_4 molecule should also be noted. The isomerization **IVa**→**IIIa** is exothermic by 15.2 kcal mol^{-1} with a barrier of 17.7 kcal mol^{-1}. The dissociation of cluster **IVa** into hydrated metaphosphate and H_3PO_4 or into water and cluster $[H_2PO_3\cdots PO_3]^-$ are endothermic by 27.0 kcal mol^{-1} and 6.8 kcal mol^{-1}, respectively.

The dissociation mechanism involving a water-assisted proton transfer to the bridging oxygen, in which one H_2O molecule acts both as a proton acceptor and donor, and which proceeds via a six-membered transition state, was also considered. Unfortunately, in this case, our theoretical investigation failed in that we were unable to locate any appropriate transition state for such a pathway; that is, analysis of its harmonic frequencies does not support assigning it a priori to the hypothesized pathway.

Finally, we also considered the dissociation of **Ia** by a direct breakage of the P–O bond, which has a length of 1.750 Å (Reaction (4)). In this extreme dissociation process, computed to be endothermic by 68.4 kcal mol^{-1}, the negative charge is transferred to the bridging oxygen atom from the oxygen bound to the terminal phosphorus atom.

$$\mathbf{Ia} \rightarrow HPO_3 + H_2O + H_2PO_4^- \qquad (4)$$

Taking into consideration the energy profiles reported in Figures 9 and 11, our energy barrier for the dissociation mechanism is slightly higher than that for the associative mechanism. It seems energetically less favorable to first break the P–O bond followed by the nucleophilic attack of the water. However, it was reported that in the $CH_3PO_3H^-$ dissociative hydrolysis, the less strained six-membered ring transition state is lower in energy than the corresponding four-membered transition state and facilitates the process.[7–8] The same influence of the water molecule was found in the $[PO_3\cdots H_2O]^-\rightarrow H_2PO_4^-$ isomerization. On the basis of these considerations and in the absence of data regarding

the active participation of the local water molecule in the transition state, we can reasonably suppose that in the gas phase the dissociative barrier of the diphosphate monoanion hydrolysis is lower than we calculated for the "classical" mechanism. For monophosphate and triphosphate ester hydrolysis the dissociative pathway is found to be more favorable than the associative pathway in the gas phase.[2] In this context, the higher activation energy of the intramolecular proton transfer to the bridging oxygen atom in the $[H_3P_2O_7\cdots H_2O]^-$ cluster (44.1 kcal mol^{-1}), than in the $H_3P_2O_7^-$ ion (36.9 kcal mol^{-1})[18] could suggest that the additional water molecule must play an active role in lowering the reaction barrier in solution.

Concerning the associative pathway shown in Figure 9, **Ia** leads directly to the linear $H_5P_2O_8^-$ ion **IIa** by passing through **TS5** (Figure 4). Our activation barrier estimate, 34.8 kcal mol^{-1}, is consistent with the previously reported values for the monophosphate and triphosphate associative hydrolysis.[2]

As we know, **IIa** can easily isomerise into **IIb** and then give **IIIa** in a barrier-free process by the breaking of the PO bond. On the other hand, our B3LYP/6-31+G* calculations failed to identify a pathway directly linking **IIa** (or **IIb**) and **IVa**, as was highlighted[2] for the hydrolysis of the protonated monophosphate methyl ester. For the $H_5P_2O_8^-$ system, the cluster **IVa** can either be reached from **IIIa** or **Ia**, but we were unable to locate any transition structure linking the linear $H_5P_2O_8^-$ clusters, group **II**, and **IVa**.

Based on theoretical results, in the CAD spectrum shown in Figure 1, it is not possible to justify the presence of the ions at *m*/*z* 97 as formed from the isomerization of cluster **I** into clusters **III** or **IV**. In fact, the barrier height for all the isomerization processes of hydrated diphosphate cluster (**I**) considered is higher than the barrier for its dissociation into $H_3P_2O_7^-$ and water.[23] Therefore, at least at our level of theory and on the basis of the isomerization pathways investigated, the hydrolysis of the diphosphate anion does not occur in the gas phase because the dissociation energy of cluster **I** is lower than all the computed isomerization barriers. Indeed, **I** may be responsible for the formation of the fragment at *m*/*z* 177, which results from the loss of the added water, but not for the fragment at *m*/*z* 97. The latter could reasonably arise from the dissociation of cluster **III**, which should already be present in the CH_4/CI plasma containing $H_4P_2O_7$ and H_2O. A viable explanation is represented by the gas-phase hydrolysis of neutral pyrophosphoric acid into phosphoric acid that occurs in the ion source. The process, $H_4P_2O_7+H_2O\rightarrow 2\,H_3PO_4$, is known to be a quasi-thermoneutral process.[12]

This hypothesis is supported by the fragmentation of the ions at *m*/*z* 197 and 209 obtained from the reaction of $H_4P_2O_7$ with labeled water or methanol. For example, the gaseous mixture arising from pyrophosphoric acid hydrolyzed by labeled water should contain H_3PO_4 and $H_3PO_3{}^{18}O$ and hence could lead to the formation of both $[H_3PO_3{}^{18}O\cdots H_2PO_4]^-$ and $[H_3PO_4\cdots H_2PO_3{}^{18}O]^-$ (cluster **III**), giving rise to the fragments at *m*/*z* 97 and *m*/*z* 99.

Analogously, the gas-phase reaction between methanol and pyrophosphoric acid (Reaction (5)) could account for the presence of the ions at *m*/*z* 97 and 111 in the CAD spectrum of the ions at *m*/*z* 209. These fragments could arise from the $[H_3PO_4\cdots CH_3OPO_3H]^-$ and $[H_2PO_4\cdots CH_3OPO_3H_2]^-$ clusters, following to the loss of methylphosphate and phosphoric acid, respectively.

$$H_4P_2O_7 + CH_3OH \rightarrow H_3PO_4 + CH_3OPO_3H_2 \quad (5)$$

In conclusion, the CAD fragments of the ions obtained from $H_4P_2O_7$ CI/CH_4 in the presence of water reflect the miscellaneous nature of this ion population. In fact, based on the computed dissociation enthalpies and the activation energies of the processes leading to the formation of the ion at *m*/*z* 177, this fragment may be said to be formed from the dissociation of clusters **I** and **IV**, two pathways requiring relatively low energies (15.4 and 6.3 kcal mol^{-1} respectively), and from the isomerization of **III** to **I**, which requires higher energy (>30 kcal mol^{-1}). In particular, this process represents the reverse energy profile of the associative mechanism shown in Figure 9. The isomerization of **III** to cluster **I** by the dissociative pathway is prevented by the loss of water from the intermediate cluster **IV**.

The fragment ions at *m*/*z* 97 can only be formed from the dissociation of cluster **III** (33 kcal mol^{-1}) because all pathways involving clusters **I** and **IV** are prevented by the easy dehydration of these species. Indeed, the fragment ions at *m*/*z* 97 are indicative of the presence of cluster **III** in the CI plasma of TQ/MS, which is formed from the gas-phase hydrolysis of neutral diphosphoric acid into phosphoric acid.

Qualitative analysis of the energy-resolved CAD spectra shown in Figure 1, shows that the ions at *m*/*z* 177 appear at energy values lower than those responsible for the appearance of the ions at *m*/*z* 97. This evidence is consistent with the presence in the CI plasma of TQ/MS of clusters **I** and/or of cluster **IV**, whose dissociation processes occur at dissociation energies lower than 33 kcal mol^{-1}.

It should be noted that both these clusters can be responsible for the fragments at *m*/*z* 177 in the CH_4/CI of phosphoric acid. In fact, cluster **IIIa**, once formed and excited by the exothermicity of its formation process, can isomerise to clusters **I** or **IV**, passing through barriers comparable in height to its dissociation barrier. In accordance with ATP generation by collisional activation of a sodiated salt cluster containing three AMP precursors,[20] the induced CAD of the $[H_3PO_4\cdots H_2PO_4]$ cluster could form the diphosphate ion.

It should be noted that clusters $[H_3PO_3{}^{18}O\cdots H_2PO_4]^-$ and $[H_3PO_4\cdots H_2PO_3{}^{18}O]^-$, found in the CI plasma of pyrophosphoric acid and labeled water, could be responsible for the loss of both labeled and unlabeled water molecules from the ions at *m*/*z* 197.

Considering that the $HP_2O_6^-$ fragment at *m*/*z* 159 was never detected in our CAD spectra, the formation of the $[H_2O\cdots HP_2O_6\cdots H_2O]^-$ cluster **V**, which, at least in principle, could allow this experimental evidence to be rationalized, can reasonably be excluded by also taking the theoretical results into account.

By analogy with the above results and considerations, it may be postulated that the same ionic species is present in the CI plasma obtained from diphosphoric acid and methanol.

It is more difficult to make a structural characterization of the ions at *m*/*z* 195 obtained from the electrospray ionization of the H_3PO_4 and $H_4P_2O_7$ solutions and investigated by the FTICR mass spectrometry. The ability of the ESI process to generate solvated species strongly suggests the $[H_3PO_4\cdots H_2PO_4]^-$ cluster structure **III** for the ions at *m*/*z* 195 arising from the H_3PO_4 solution. The ions at *m*/*z* 195 are present at very low intensities in the ESI spectrum of $H_4P_2O_7$ solution and are absent in the ESI spectra of $Na_4P_2O_7$ and $Na_5P_3O_{10}$ solutions, although they display ions at *m*/*z* 177. This evidence seems to suggest the influence of solution pH and indeed of the presence of H_3PO_4 in determining the formation of the $[H_3PO_4\cdots H_2PO_4]^-$ cluster. However, the presence of the $[H_3P_2O_7\cdots H_2O]^-$ cluster structure **I** or $[H_3PO_4\cdots PO_3\cdots H_2O]^-$ cluster structure **IV** cannot be definitively excluded.

In conclusion, the different nature of the ionic formation process, the absence of energy-resolved CAD spectra, and the lack of specific structurally diagnostic fragments do not allow any definitive conclusion to be drawn regarding the connectivity of $H_5P_2O_8^-$ ions investigated by FTICR mass spectrometry. Moreover, the study of $H_5P_2O_8^-$ ion reactivity, which could represent a useful probe for the structural characterization of these ions, is unfortunately limited by their low reactivity. The $[H_3PO_4\cdots H_2PO_4]^-$ cluster was found to exhibit broader reactivity than the analogous monomeric ion in the reaction with trimethylborate.[25] In this work the only reaction observed using trifluoroacetic acid provided no definitive evidence on the structure of $H_5P_2O_8^-$ ions. On the basis of gas-phase acidity values[22,23] and by disregarding the fact that these thermochemical data are referred to non-solvated species, proton transfer leading to the CF_3COO^- ions should involve clusters containing $H_2PO_4^-$, which is more likely than the $H_3P_2O_7^-$ moiety. Furthermore, the simplest hypothesis to justify the formation of the $[CF_3COOH+H_2PO_4]$ addition product is based on the ligand-exchange reaction involving cluster **III**. However we cannot exclude different pathways leading to the elimination of a phosphoric acid molecule.

Conclusions

The ionic population of gaseous $H_5P_2O_8^-$ ions obtained from CH_4/CI of $H_4P_2O_7$ and water was structurally assayed by CAD TQ mass spectrometry. Theoretical calculations performed at the B3LYP/6-31+G* level of theory allowed the rationalization of the origin of CAD fragments and the structural characterization of the gaseous $H_5P_2O_8^-$ as a mixture formed by $[H_3P_2O_7\cdots H_2O]^-$, $[H_3PO_4\cdots H_2PO_4]^-$, and $[PO_3\cdots H_3PO_4\cdots H_2O]^-$ clusters. This study provides a consistent picture of the previously unexplored gas-phase ion chemistry of $H_5P_2O_8^-$ ions and uses theoretical methods to examine the gas-phase hydrolysis and synthesis mechanisms of diphosphate ion.

Experimental Section

Materials: H_3PO_4, $H_4P_2O_7$, $Na_4P_2O_7$, $Na_5P_3O_{10}$, $H_2{}^{18}O$ (99 atom%), and all chemicals were purchased from Sigma Aldrich Ltd. and used as received.

Instrumentation: ESI-FTICR/MS experiments were performed with a Bruker BioApex 4.7T FT-ICR mass spectrometer equipped with an Analytica of Brandford electrospray ionization source. Samples were infused into a fused-silica capillary (i.d. 50 m) at a flow rate of 130 L min^{-1} and the ions were accumulated in a hexapole ion guide for 0.8 s. Typical ESI voltages for cylinder, capillary, and end plates are 3000, 4000, and 4300 V respectively. The capillary exit and skimmer voltages are set to −60 and −10 V, respectively, and the hexapole d.c. offset to 0.7 V.

Triple quadrupole mass spectra were recorded on a TSQ 700 mass spectrometer from Finnigan Ltd operating in the negative-ion mode.

Methods: In the FT-ICR experiments, ESI solutions were prepared daily at a concentration of 10^{-4} M by dissolving H_3PO_4, $H_4P_2O_7$, $Na_4P_2O_7$, or $Na_5P_3O_{10}$ in acetonitrile/water (1:1) and were used immediately for analysis. The $H_5P_2O_8^-$ ions were obtained from a CH_3CN/H_2O (1:1) solution of $H_4P_2O_7$ or H_3PO_4. The $H_5P_2O_8^-$ ions were transferred into the resonance cell (25 °C) and isolated by broad-band and "single-shot" ejection pulses. After a thermalising delay time of 1–2 s, the ions were re-isolated by "single shots" and allowed to react with neutral reagents in the cell.

In the triple quadrupole (TQ) mass spectrometric experiments, H_3PO_4 or $H_4P_2O_7$ were introduced into the ionic source by a direct insertion probe maintained at 200 °C by thermostat. The $H_5P_2O_8^-$ ions were generated by chemical ionization (CI) of $H_4P_2O_7/H_2O/CH_4$ or H_3PO_4/CH_4 mixtures. The ions of interest were isolated by the first quadrupole (Q1) and driven into the collision cell, actually an RF-only hexapole, containing the neutral reagent at pressures up to 1 mTorr. Collisionally activated dissociation (CAD) experiments are recorded using Ar as the target gas at a pressure of $1–5\cdot10^{-5}$ Torr and at a collision energy ranging from 0 to 50 eV (laboratory frame). The charged products are analyzed with the third quadrupole, scanned at a frequency of 150 amu s^{-1}.

Computational details: Density functional theory based on the hybrid[24] B3LYP functional,[25] was used to localize the stationary points on the investigated potential energy surface. This functional is based on the Becke three-parameter functional, which includes a Hartree–Fock exchange contribution. It comprises the nonlocal correction for the exchange potential proposed by Becke in 1988 together with the nonlocal correction for correlation energy provided by the functional of Lee, Young, and Parr. Thermochemical calculations were carried out at 298.15 K and 1 atm by adding the zero-point correction and the thermal correction to the calculated B3LYP energies. The correctness of using density functional calculations for the treatment of negative ions has been exhaustively reviewed.[26] The absolute entropies were calculated using standard statistical-mechanistic procedures from scaled harmonic frequencies and moments of inertia relative to the B3LYP/6-31+G* optimized geometries. The 6-31+G* basis set was used.[27] This presents a good compromise between accuracy and saving in computational resources. All calculations were performed using the program Gaussian 98.[28]

Acknowledgments

The authors again wish to express their gratitude to the late Professor Fulvio Cacace, for his teaching and the enthusiasm for research which he transmitted with such great patience and affection. Financial support from the Italian Ministero dell'Università e della Ricerca Scientifica e Tecnologica (MURST) is gratefully acknowledged.

[1] F. H. Westheimer, *Science* **1987**, *235*, 1173.
[2] Y.-N. Wang, I. A. Topol, J. R. Collins, S. K. Burt, *J. Am. Chem. Soc.* **2003**, *125*, 13265, and references therein.
[3] J. Akola, R. O. Jones, *J. Phys. Chem. B* **2003**, *107*, 11774.
[4] S. D. Lahiri, G. Zhang, D. Dunaway-Mariano, K. N. Allen, *Science* **2003**, *299*, 2067.

[5] P. K. Grzyska, P. G. Czyryca, J. Purcell, A. C. Hengge, *J. Am. Chem. Soc.* **2003**, *125*, 13106, and references therein.
[6] J. Florian, A. Warshel, *J. Phys. Chem. B* **1998**, *102*, 719.
[7] C.-H. Hu, T. Brinck, *J. Phys. Chem. A* **1999**, *103*, 5379.
[8] M. Bianciotto, J.-C. Barthelat, A. Vigroux, *J. Am. Chem. Soc.* **2002**, *124*, 7573, and references therein.
[9] a) J. Florian, A. Warshel, *J. Am. Chem. Soc.* **1997**, *119*, 5473; b) J. Aqvist, K. Kolmodin, J. Florian, A. Warshel, *Chem. Biol.* **1999**, 6R71; c) H.-J de Jager, A. M. Heyns, *J. Phys. Chem.* **1998**, *102*, 2838.
[10] S. J. Admiraal, D. Herschlag, *J. Am. Chem. Soc.* **2000**, *122*, 2145.
[11] T. M. Glennon, J. Villà, A. Warshel, *Biochemistry* **2000**, *39*, 9641.
[12] a) H. Saint-Martin, I. Ortega-Blake, A. Les, L. Adamowicz, *Biochim. Biophys. Acta* **1991**, *1080*, 205–214; b) H. Saint-Martin, I. Ortega-Blake, A. Les, L. Adamowicz, *Biochim. Biophys. Acta* **1994**, *1207*, 12–23; c) T. Johnson, J. R. Panas, *J. Chem. Phys.* **2002**, *116-117*, 45.
[13] a) B. Ma, C. Meredith, H. F. Schaefer, III, *J. Phys. Chem.* **1994**, *98*, 8216; b) M. E. Colvin, E. Evleth, Y. Akacem, *J. Am. Chem. Soc.* **1995**, *117*, 4357.
[14] H. Saint-Martin, L. E. Ruiz-Vicent, A. Ramìrez-Solìs, I. Ortega-Blake, *J. Am. Chem. Soc.* **1996**, *118*, 12167.
[15] B. Ma, C. Meredith, H. F. Schaefer III, *J. Phys. Chem.* **1995**, *99*, 3815.
[16] W. J. McCarthy, D. M. A. Smith, L. Adamowicz, H. Saint-Martin, I. Ortega-Blake, *J. Am. Chem. Soc.* **1998**, *120*, 6113.
[17] H. Saint-Martin, L. E. Vicent, *J. Phys. Chem. A* **1999**, *103*, 6862.
[18] A. Ricci, F. Pepi, M. Di Stefano, M. Rosi, *Chem. Eur. J.* **2004**, *10*, 840.
[19] A. T. Blades, Y. Ho, P. Kebarle, *J. Am. Chem. Soc.* **1996**, *118*, 196; b) R. G. Keese, W. Castleman, Jr., *J. Am. Chem. Soc.* **1989**, *111*, 9015; c) B. Ma, Y. Xie, M. Shen, H. F. Schaefer III, *J. Am. Chem. Soc.* **1993**, *115*, 1943.
[20] R. Julian, J. L. Beauchamp, *Int. J. Mass Spectrom.* **2003**, *227*, 147, and references therein.
[21] S. Gronert, R. A. O'Hair, *J. Am. Soc. Mass Spectrom.* **2002**, *13*, 1088.
[22] NIST Chemistry WebBook; NIST standard Reference Database No 69 - February **2000** release; data collection of the National Institute of Standards and Technology to be found under http://webbook.nist.gov.
[23] $\Delta H°_{acid}$ ($H_4P_2O_7$) = 323 kcal mol^{-1},[13] $\Delta H°_{acid}$ (H_3PO_4) = 344 kcal mol^{-1},[22] $\Delta H°_{acid}$ (HPO_3) = 303 kcal mol^{-1},[22] $\Delta H°_{acid}$ (CF_3COOH) = 323 kcal mol^{-1}.[22]
[24] A. D. Becke, *J. Chem. Phys.* **1993**, *98*, 5648.
[25] A. D. Becke, *Phys. Rev. A* **1988**, 38, 3098; b) C. Lee, W. Yang, G. G. Parr, *Phys. Rev. B* **1988**, 37, 785.
[26] J. C. Rienstra-Kiracofe, G. S. Tschumper, H. F. Schaefer III, *Chem. Rev.* **2002**, *102*, 231.
[27] M. J. Frisch, J. A. Pople, J. S. Binkley, *J. Chem. Phys.* **1984**, *80*, 3265, and references therein.
[28] M. J. Frisch, G. W. Trucks, H. B. Schlegel, G. E. Scuseria, M. A. Robb, J. R. Cheeseman, V. G. Zakrzewski, J. A. Montgomery, R. E. Stratmann, J. C. Burant, S. Dapprich, J. M. Millam, A. D. Daniels, K. N. Kudin, M. C. Strani, O. Farkas, J. Tomasi, V. Barone, M. Cossi, R. Cammi, B. Mennucci, C. Pomelli, C. Adamo, S. Clifford, J. Ochterski, G. A. Petersson, P. Y. Ayala, Q. Cui, K. Morokuma, D. K. Malick, A. D. Rabuck, K. Raghavachari, J. B. Foresman, J. Cioslowski, J. V. Ortiz, B. B. Stefanov, G. Liu, A. Liashenko, P.Piskorz, I. Komaromi, R. Gomperts, R. L. Martin, D. J. Fox, T. Keith, M. A. Al-Laham, C. Y. Peng, A. Nanayakkara, C. Gonzalez, M. Challacombe, P. M. W. Gill, B. G. Johnson, W. Chen, M. W. Wong, J. L. Andrei, M. Head-Gordon, E. S. Replogle, J. A. Pople, Gaussian 98 (Revision A.1), Gaussian, Inc., Pittsburgh, PA, **1998**.

Received: March 25, 2004
Published online: October 7, 2004

